Wettability of Electrospun Poly(vinylpyrrolidone)−Titania Fiber Mats on Glass and ITO Substrates in Aqueous Media

Jamie M. F. Jabal, Laurel McGarry, Abigail Sobczyk, and D. Eric Aston*

Department of Chemical & Materials Engineering, P.O. Box 441021, University of Idaho, Moscow, Idaho 83844-1021

ABSTRACT Networks of nano/microfibers (fiber mats) have been electrospun from solutions of dispersed poly(vinylpyrrolidone) (PVP) and a titania precursor onto glass and indium−tin oxide (ITO) plates to study their wettability. Collection time and electrode separation are the two key fabrication parameters investigated, along with the flow rate, polymer molecular weight, and drying conditions, to determine the effects on network morphology and the relationship to contact angles. Measurements indicate that the fiber mats on both glass and ITO increase in thickness and contact angle for longer spinning time and shorter distance, resulting in an extreme case of apparent ultrahydrophobicity on ITO of up to 169.9° with water. The fiber mats are shown by optical microscopy to exhibit differences in morphology for insulating glass (straight) and conductive ITO (loopy) substrates responsible for the wide-ranging and well-controlled wettability to within 1−2°. Fiber mats baked at 200 °C for 24 h show excellent mechanical stability with wetting even against frequent heavy rinsing, conducive for reusable aqueous applications such as biosensors or cellular scaffolding.

KEYWORDS: electrospinning • nanofibers • microfibers • titania • poly(vinylpyrrolidone) • contact angle

INTRODUCTION

Electrospinning is an effective tool in the fabrication of microfibers, nanowires, nanofibers, and other nanostructures for various applications. This century-old method has been modified by many researchers for the nanofabrication of a variety of materials, such as polymer-based nanofibers, composites, and ceramics (1−3). Compared to most other methods, it has a simple yet versatile setup that produces a significant amount of ultrafine fibers in the diameter range of a few micrometers down to tens of nanometers in a short period of time. Electrospinning is also well-suited for forming fiber assemblies on a wide variety of substrates, generally arranged in a pseudorandom or chaotic manner. Other advantages include the ease of room temperature deposition and a wide range of precursor materials available for synthesis via this method. It makes use of electrostatic forces to stretch a polymer-based solution as it solidifies, wherein a poly(vinylpyrrolidone) (PVP) shell surrounding the nanofiber is shown on SEM images (4). The setup can be customized to collect oriented nanofibers as nonwoven mats, ordered "nano-grooves" (5), single nanowires across specific electrodes (6), or nanofiber yarn (1). The disadvantages of this method are limited to the area of collection and the reported setup modifications, which may cause the following unwanted changes in the fiber mats (1): thickness of the fiber layers, fiber breakage, lengths of the fibers (3), or alignment of the fibers. The large surface-to-area ratio of nano- and microfibers has improved the performance in a variety of applications, such as chemical and biological sensors, tissue engineering, protective clothing, and wastewater treatment (5).

Although others have used silicon (5), gold (1, 7), and molybdenum nanowires (1, 8), or aluminum nanofibers (1, 9), titania is still widely chosen for an electrode material in environmental, medical, and sensing applications, viz., all aqueous applications. Electrospun titania nanofibers have been studied on various substrates: gold electrodes (7−9, 11), stainless steel (17, 19), alumina plates (18), and aluminum foil (1−6, 27), all exhibiting loopy or chaotically coiled fibers. Titania nano- and microfibers appeared straighter and more aligned across copper grids (12) and silicon nitride membranes (13, 15, 20). The average diameters of the fibers ranged from 20 to 200 nm, and lengths were up to several centimeters. In all of these cases, PVP was the polymer used, which is a key ingredient to host the specific precursor for the type of fiber to be spun. Others have used matrix polymers such as poly(vinyl alcohol), poly(aniline) (29), or poly(ethylene oxide) (PEO) (21−23). Baking the electrospun materials at high temperatures ranging from 200 to 500 °C (2−7, 17−19, 27) can remove the polymer without destroying the porous structures of the fiber constructions (4, 13, 14). Even at lower temperatures, this enhances the mechanical strength of the fiber networks by softening the polymer coating enough to fuse contacting segments. Higher temperatures can promote annealing of the titania fibers and possibly eliminate organic components without destroying the nanostructure of the fibers (18).

Encapsulation of various functional components into the electrospun fibers has been studied by several researchers as well (24−31). Nanotubes improve the mechanical strength

* E-mail: aston@uidaho.edu.
Received for review July 20, 2009 and accepted September 25, 2009
DOI: 10.1021/am900481d

and electrical conductivity of the fibers (4). Carbon, titania, silver, and iron oxide nanoparticles have also been added to fibers for different functions (5, 8, 13, 14, 17). Titania nanofibers, which were cobalt-doped, exhibited a ferromagnetic characteristic that is useful for magnetic applications (14). In addition to this, molecular species such as DNA (22), enzymes (30), and drugs (31) are encapsulated for another function of these fibers. DNA is encapsulated from an aqueous solution by using PEO to improve the biocompatibility of the electrospinning solution (21, 22). Nanofibers containing an active enzyme and polymer are electrospun directly from their mixture in an organic solvent (23, 30). Titania nanomats are also used for antimicrobial purposes by using titania's natural properties of photocatalysis (18). In the biomedical field, drugs are easily captured within the structure of electrospun fibers and can be delivered either transdermally (i.e., tissue engineering), by injection, or by implantation (30, 31). Electrospun nanofibers have also shown a compatible environment for cell growth. Cells cultured on aligned nanofiber scaffolds have been shown to proliferate in the direction of the fiber orientation (32).

The objective of this paper is to demonstrate the ability to fabricate a PVP—titania composite fiber mat and to control the degree of wettability for aqueous applications without changing the chemical nature of the material. In order to address a broad range of utility, electrospinning is accomplished on the relatively inexpensive surfaces of indium—tin oxide (ITO)-coated glass and microscope glass slides. The selection of substrates was made based on the similarity of the surface roughness and commercially available dimensions, on the ultrahigh transmissivity of visible light and commonality of laboratory use for future incorporation into biological applications, and on their distinct differences in surface conductivity and wettability before coating with fiber mats. This study focuses mainly on the effects of electrode separation and spinning time on the contact angle for these two substrate cases. Both water and a cell culture media solution (DMEM) were used to ensure that there were no significant differences in the fiber mat wettability for cellular applications.

MATERIALS AND METHODS

Electrospinning System. Titania—composite fiber networks were fabricated using the electrospinning method of applying a large electrical potential difference between a dosing syringe needle and a conductive substrate to form fine fibers (micro- and nanoscale diameter range) that collect into a chaotic mat (1—14). The setup consists of a syringe pump (Advance Series 1200), a high-voltage direct-current (dc) unit (HVPS, EMCO High Voltage Corp.), and a 1-mL syringe with a 27 G 1 $^1/_4$-in. metallic needle (BD Medical-Becton, Dickinson, and Company) (Figure 1). Initially, one syringe was used for preparing fiber mats, but all data reported herein were gathered from dual-syringe fabrication with a distance of 1.5 cm between the needles. Multiple syringes reduce the electrospinning time for a particular amount of fiber mat produced (1); however, two syringes were a practical limit for the current setup. Using two syringes compared to one (used initially) showed a decrease in the collection time, thus providing an increased amount of sample produced in time. In a typical electrospinning set-up, the voltage applied is more than 5 kV (1). The voltage unit and dual-syringe design

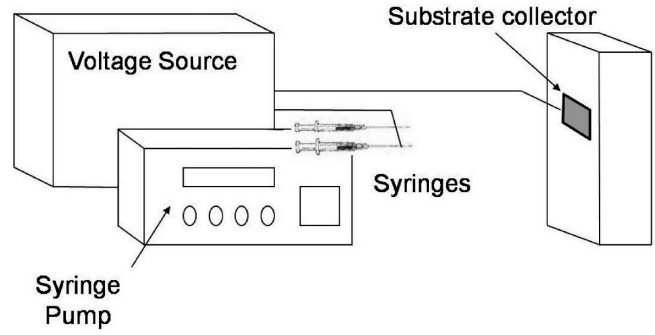

FIGURE 1. Electrospinning schematic.

operated at an 8-kV potential difference for all substrates, flow rates, electrode spacing (i.e., collection distance), and solution formulations in order to hold a consistent, steady-state fabrication regime for a wide range of parameters at well below the voltage source limit. In this manner, the electric field is controlled via the collection distance while keeping the electrode dimensions constant.

Chemicals. The following chemicals were used for the titania-composite electrospinning solution: glacial acetic acid (Fisher Scientific); 200 proof ethyl alcohol (AAPER Alcohol & Chemical Co.); poly(vinylpyrrolidone) (PVP) of 1 300 000 molecular weight (Sigma-Aldrich CAS 9003-39-8); titanium(IV) isopropoxide (Fluka and Sigma-Aldrich) as the titania precursor. Three different molecular weights of PVP were initially investigated for feasibility: 58 kDa, 360 kDa, and 1.3 MDa.

Substrates. The substrates tested were standard biological glass slides (as received) and indium—tin oxide (ITO) plates (Delta Technologies Ltd.) supported on SiO_2-passivated, unpolished float glass. The surface conductivity of these ITO plates are 0.010—0.014 S/m, according to the manufacturing data. Both substrates were used without prior rinsing or cleaning. ITO plates are precut by the manufacturer to a measurement of 18 × 25 × 1.1 mm^3; glass slides are cut in the lab to a measurement of 20 × 25 × 1.1 mm^3 and centered on a 30 × 25 mm^2 piece of aluminum foil. The ITO surface is the grounded spinning electrode, while the insulating glass is backed with the larger conducting foil to attract the electrospun fibers in the substrate direction.

Collection Distance and Time. All fiber mats for quantitative analysis were produced at a syringe pump flow rate of 10 μL/min, typical for others reported (1); however, flow rates above and below this level were also explored. The fibers were collected for four distances as measured from the tip of the syringe needle to the substrate: 5, 10, 15, and 20 cm. The collection distances reported range from 4 to 14 cm (11). The times for collecting fibers on the substrates were 3 s, 5 s, 10 s, 20 s, 1 min, 5 min, and 10 min, similar to those in the literature (1—11).

Fabrication of Fiber Mats. Combining acetic acid, ethanol, PVP, and titanium precursor makes a polymer/sol—gel solution to be loaded into the syringes (13, 25). PVP is soluble in alcohols and compatible with titanium precursors, while acetic acid stabilizes and controls the hydrolysis reaction of the solution (14). First, combining the following chemicals in a small vial makes solution A: 2.5 mL of ethanol and 0.15 g of PVP. The vial is placed in a sonicator (Sharpertek) for 30 min to allow PVP to disperse well. Then, solution B is made in another small vial by mixing 0.52 mL of the titanium precursor, 1 mL of acetic acid, and 1 mL of ethanol and stirring for 10 min. Solution B is slowly poured into solution A and stirred for 1 h.

Initially, solution A appears clear and solution B appears clear with a very pale-yellow tint. When both solutions are mixed, the solution immediately turns a more distinct light-yellow color. This yellow color is exhibited by the titania precursor mixing

with ethanol. The resultant titania-spinning solution is loaded into syringes for synthesis.

An unused solution is ideally viable for 2−3 days while continuously stirred to prevent solidification. The solution gradually turns cloudy yellow to cloudy white by the fourth day, which suggests that the constituents are no longer dispersed uniformly enough to form the desired fibers. The solution remains a cloudy white color past 4 days as the titania gradually precipitates more and larger crystals unsuited for electrospinning.

Electrospinning is done at room temperature in order for the metal alkoxides to hydrolyze by reacting with moisture in the air to create a network within the polymer (1−8, 25−27). At a specific flow rate of 10 μL/min, the syringe pump is programmed to drive the titania solution to the needle tip and form a droplet. The HVPS is then turned on at 8 kV between the paired needles and the substrate; glass slides are placed on a piece of grounded aluminum foil, while the ITO plates are directly grounded.

The solution droplet stretches into a structure called the Taylor cone (3−7). Eventually, an electrified liquid jet forms, elongates, whips continuously because of transient electrostatic events imposed by the dc potential, and deposits at the grounded collector. This startup to steady-state electrospinning takes about 3 s, after which the fabrication time for the fiber mat is counted. The jet can be stretched to nanometer-scale diameters, with some modicum of control through the electrospinning parameters and solution conditions because of a combined effect of the whipping caused by bending instabilities in the electrified jet and the solvent evaporation. The substrates with the electrospun titania fibers are then baked in a standard laboratory oven (VWR International) at 200 °C for 24 h to fuse the network into a rigid mat against the capillary forces of aqueous environments (25). All images are captured with a CCD camera attached to an optical microscope (Olympus BX51), under autoexposure using an objective magnification of 20× in dark-field mode.

Wettability. The contact angles of NANOPure water (Barnstead NANOPure Infinity System) and Dulbecco's Modified Eagle Media (DMEM) with the substrates and electrospun fiber mats before and after baking were measured using a Ramé-Hart goniometer. Five samples of each parameter set were measured in five different areas on each sample: the center and four quadrants. The experimental errors reported are the standard deviations of the replicated measurements, and there is an instrument error of 0.5°. The substrates used were tested as-received without any cleaning procedure. Hydrophobic surfaces are partially nonwetting and considered to have contact angles between 90° and 180°, while hydrophilic surfaces are partially wetting between 0° and 90° (21). It is common, however, to distinguish the partial wettability in materials exhibiting higher apparent angles, e.g., 60−89°, where the behavior of interest in aqueous media is substantially different from more highly wetting cases, e.g., 10−30°, even though both example ranges are hydrophilic by definition. While no formal definitions along these examples have been fully established and accepted, it is, nevertheless, more convenient herein to make such distinctions in both hydrophobic and hydrophilic regimes.

RESULTS AND DISCUSSION

Initially, we used 58 and 360 kDa PVP, which resulted in weak, broken fibers on both glass and ITO substrates. These lower molecular weights were initially used to explore the range of effects on the titania fiber formation because there is motivation for their use to reduce viscous losses in future scale-up; however, the shorter polymer chains were not found to be suitable for consistent and long fiber formation in networks. The 58 and 360 kDa PVP tended to splatter dots of polymer−titania mixtures onto the substrates instead of pure fiber mats. These findings on the dual-syringe process further support the extended literature in the preferred use of higher molecular weight PVP (1, 2, 5, 8, 10, 13) to reduce beading and to spin stronger fibers over the electrodes. There is specific evidence that the 1.3 MDa PVP gives the fiber its shape once ejected from the tip of the needle (3, 8−10, 38).

The fiber mats of this quantitative study were formed at 8 kV and separations from 5 to 20 cm, or electric fields of 1.6−0.4 kV/cm, with very consistent trends in morphology (Tables 1 and 2). While the majority of the fibers exhibit diameters in the range of 2−5 μm, about 20% are half a micrometer or less. The thickest fiber mats have a thickness of about 200 μm. In comparison, the thinnest fiber mats from previous studies were generated by a 1.6 kV/cm field (8 kV at 5 cm) (14). Various researchers have applied a range of 1−3.3 kV/cm (1, 14). Here, a thin layer of fiber mats formed on the surface of glass and ITO. The wires started to form at 5 kV, as was also reported by others (1, 14), but at 10 kV, the electrospinning started to clog the needle at all electrode distances.

The most significant change in the fiber mats after baking was the yellowing color. The as-spun fiber mats are initially white. The images of the fiber mats on both ITO and glass (Tables 1 and 2) appear to have varying yellowish colors attributed to the automatic adjustment of the CCD and the different light levels. All samples have similar characteristic yellowish color.

Fibers were easily collected on both substrates at the shortest distance and time of 5 cm and 3 s. After 1 min, surfaces of both glass (Table 1) and ITO (Table 2) had grown fiber mats thick enough to obscure most of the underlying substrate area. Collecting for yet longer times (5 and 10 min) at shorter distances shows few obvious differences in the overall morphology other than greatly thickening the layer of fibers. All fiber mats show some degree of nonuniformity; however, there is a clear trend in the trade-off of time and distance for the lateral density and mat thickness.

The most notable qualitative difference between glass and ITO is the nature of the individual fiber shape. The insulating glass substrates collect mats of very straight fibers (Table 1), while the ITO mats exhibit generally more loopy fiber mats with some extremely tortuous fiber examples visible in the micrographs (Table 2). The exposed perimeter of the aluminum foil used behind the glass substrates acted as the conductive counter electrode, and the glass collected the fibers whipping across its insulating gap from one side of the foil to another. The fibers on the perimeter of the glass are perpendicular to the edges. The straighter morphology of the fiber indicates the collection of the electrospun fibers over a gap formed between two conductive substrates. As a result of electrostatic interactions, the fibers were stretched to form a parallel array across the gap (11). The ITO surface is very conductive so the long fibers tend to form loops when attracted to the surface. The straight path of the jet is

Table 1. Optical Images (20×) of Electrospun Titania Fiber Mats on Glass Slides with Variable Collection Distance and Time

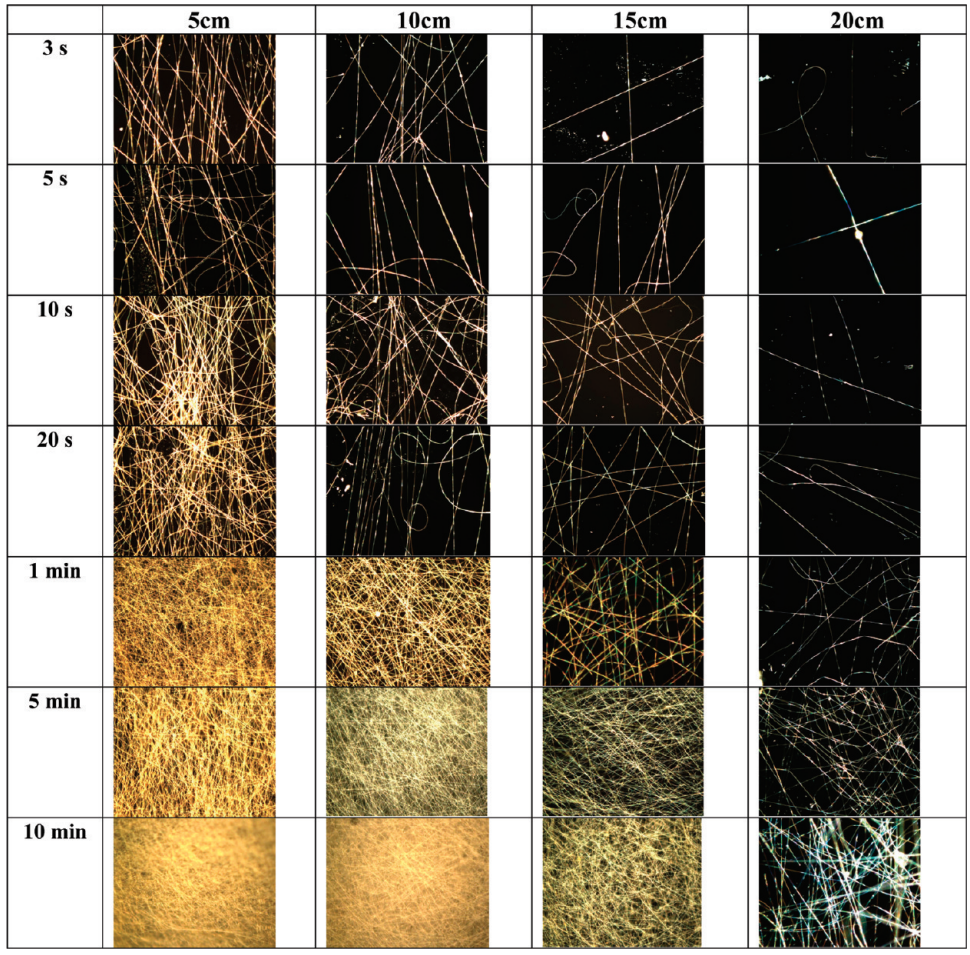

followed by a series of coils of increasing diameters that lead to an electrical bending instability, forming smaller coils (43).

As expected, the accumulated fiber mats are less dense for larger collection distances, and it takes more time for the fiber mats to collect on the substrates. Increased electrode–needle distances of 10–20 cm cause more of the fibers to deposit onto the laboratory bench as a result of gravity before reaching the electrode (23–27). When the collection times were shorter than 1 s, only a small number of nanofibers (no microfibers) were deposited across the gap, similar to previous work (1–3, 28–30). These fibers tend to be well separated from each other because of repulsive interactions between the residual charges on their surfaces (11, 32). It is interesting to note that the fiber mats are less dense laterally for longer distances, regardless of their total thickness. The more dense fiber mats formed at a distance of 5 cm. At this distance, thick fiber mats started to appear on glass at 1 min compared to ITO, wherein the thick fiber mats already formed at 20 s.

Thicker fiber mats were collected with glass and ITO at syringe flow rates of 10 μL/min compared to 1.0 μL/min, as expected (1). A further nuance to the morphology is that the thicker mats spun from a 10 μL/min flow rate have generally thinner diameter wires visible in the uppermost layers, especially at shorter collection distances (5–10 cm). The distance observation agrees with other studies that found a 5-cm distance to produce the finest wires. The diameters of the fibers on ITO are between 100 and 800 nm (Figure 2). The nonconducting glass exhibits straighter but fewer fibers on the surface than on ITO (conducting). Flow rates lower than 0.5 μL/min pump insufficient amounts of solution to produce a proper electrospinning jet, and flow rates higher than 10 μL/min pump too much solution, which creates beading within the fibers (1–3, 21, 25, 30).

Wettability. The wettability of as-received glass substrates without fiber mats shows a much lower range in contact angles than ITO plates (Table 3). Ideally, glass should have a contact angle of 0° (21), but it has been reported that cleaned glass has contact angles that range from 30 to 64° (39, 40). ITO plates that have been cleaned in detergent, rinsed in acetone, and dried in nitrogen are reported to have contact angles in the range of 65–67° (41, 42). Slight differences in contact angles for DMEM may be expected because of its various constituents, which are inorganic salts, amino acids, vitamins, and phenol red dye (CAS 143-74-8). They appear here to remain well within experimental error.

The wettability of the substrates with electrospun titania fiber mats shows contact angles monotonically increasing with coverage for both substrates. Most prominent effects

Table 2. Optical Images (20×) of Electrospun Titania Fiber Mats on ITO Plates with Variable Collection Distance and Time

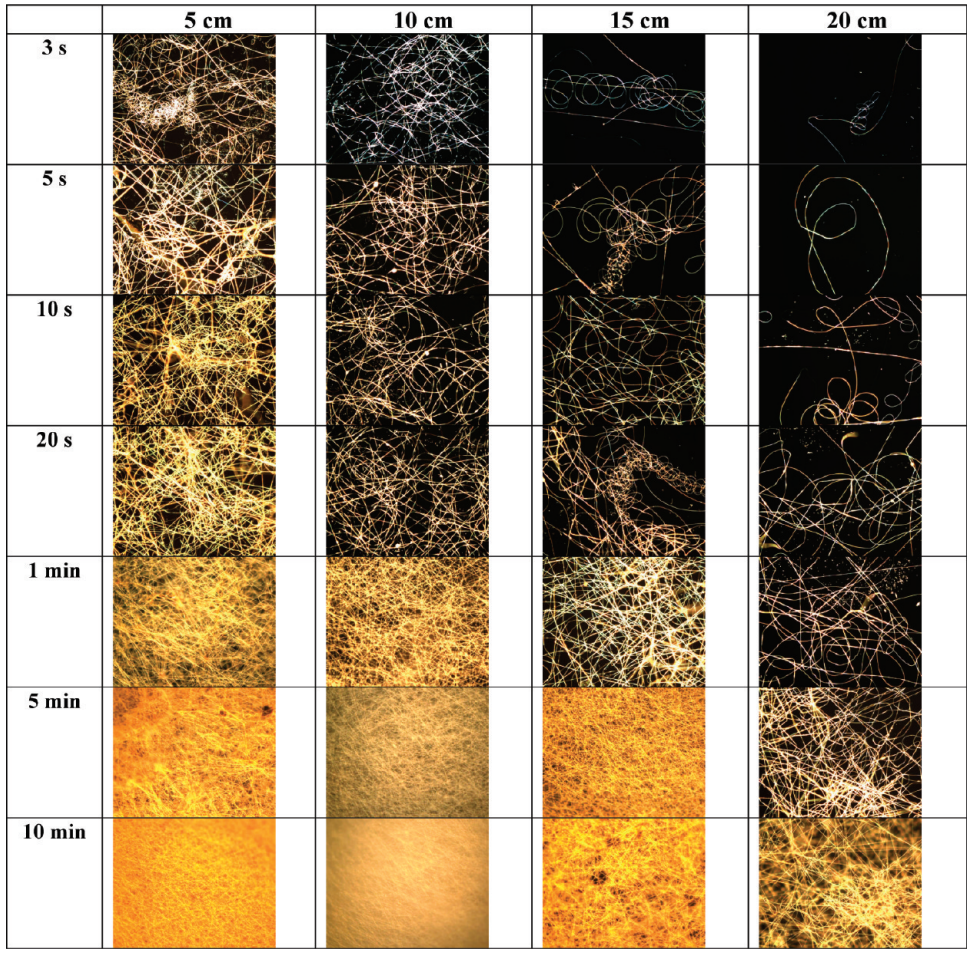

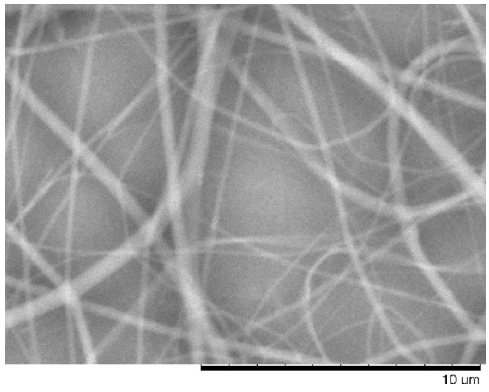

FIGURE 2. SEM image of titania fiber mats on ITO (10 000×) electrospun at 5 cm for 5 s.

Table 3. Wettability of Glass and ITO Tested with Water and DMEM Cell Media

	contact angle (deg)	
substrate	H_2O	media
glass slides	15.6 ± 0.7	16.2 ± 0.8
ITO plates	90 ± 0.5	89.4 ± 0.5

are caused by baking of the fiber mats, which was initially accomplished at 150 °C for 16 h, with some success toward increasing their mechanical stability in an aqueous environment (Table 4). All contact angles increased after baking, but once subjected to water or media, the fiber mats broke apart on the surface of the glass. The fiber mats on the ITO were slightly affected, with similar and undesirable disruption of the network structure. This is due to the hydrophilic PVP coating of the fibers that remain vulnerable to the water disjoining the contact points (11, 14). When subjected to liquid, the thicker fiber mats tend to absorb and wick into other areas, particularly when droplets are placed at the fiber edges for glass but again not for ITO. As for the thinner fiber mats, the liquid tends to remain in regions of loopy fibers that are mostly found on ITO.

Table 4. Wettability of PVP–Titania Fibers Electrospun at 5 cm for 5 s and Dried below and above the Glass Transition Temperature

		contact angle (deg)	
substrate	dry time (h)/temp (°C)	H_2O	media
glass	16/150	20.4 ± 0.5	21.9 ± 0.5
glass	24/200	79.3 ± 0.8	84.4 ± 0.5
ITO	16/150	128.5 ± 0.5	126.4 ± 0.5
ITO	24/200	140.6 ± 0.5	137.4 ± 0.5

An increased baking temperature of 200 °C, at the lower end of the typical range of 200–500 °C (2–7, 17–19, 27), was then used for 24 h to compare the mechanical stability

of the fiber networks (Table 4). The melting point of 1.3 MDa PVP is 330 °C, and its glass transition temperature (T_g) is 178 °C (39). Therefore, baking at 200 °C was expected to provide enough softening to promote stronger adhesion of the fiber mats to each other and at the interfaces of the substrates. After observation of the weak fiber network produced at a baking temperature of 150 °C for 16 h, all samples were baked only at 200 °C for 24 h.

The resulting PVP–titania mats strongly adhere to each other and to both substrates without damage because of contact angle measurements and further remain intact against very heavy rinsing streams. While there are substantial increases in contact angles for the ITO-supported networks, the greatest increases are observed for the glass samples. On the basis of comparisons in the fiber mat breakup between the two substrate types, it appears that having the ITO directly grounded for electrospinning promoted better fiber contact with the surface initially. Samples covered and stored for 3 months in ambient air showed consistent wettability, further suggesting that prolonged exposure to normal moisture conditions does not have an obvious impact.

A thorough wettability study of fiber mats processed at 200 °C demonstrates the fine level of control that can be accomplished as a function of the electrospinning collection distance and time (Table 5). It is quite feasible to prepare a PVP–titania network of essentially any apparent contact angle required above that of the underlying substrate with a precision of about 1° and a very tight areal distribution across the mat. As expected, the contact angles increase with the collection time and decrease with the distance. For any given distance, the fibers collected at both 3 and 5 s exhibit little change in contact angles because the surface coverages and layering morphologies are very similar (Tables 1 and 2). For collection times up to 1 min, the resulting contact angle increases the most with the fiber mat thickness. Much longer times of 5 and 10 min greatly increase the thickness but have much less effect on the contact angle. The overall contact angles are lower for glass than for ITO at all conditions, which suggests the curious conclusion that the morphologies of even the very thick mats (e.g., hundreds of micrometers) are significantly different and dependent on the substrate. Furthermore, the ITO as a substrate clearly encourages the formation of so-called ultrahydrophobic surfaces, which is mostly attributed to the nature of the morphology rather than the inherent hydrophobicity of the constituent material (44, 45). The apparent contact angles greatly exceed expectations for thick PVP-coated titania fiber mats.

Table 5. Contact Angles (deg) of PVP–Titania Fiber Mats on Glass and ITO Baked at 200 °C for 24 h

distance (cm) + time	glass	ITO plates
5 + 3 s	79 ± 0.7	137.7 ± 0.5
5 + 5 s	79.3 ± 0.8	140.6 ± 0.5
5 + 10 s	98.6 ± 1.2	149.8 ± 0.8
5 + 20 s	107.6 ± 0.5	155.2 ± 0.8
5 + 1 min	115.6 ± 0.5	159.5 ± 0.5
5 + 5 min	118.3 ± 0.5	162.9 ± 0.3
5 + 10 min	120.9 ± 0.3	169.9 ± 0.3
10 + 3 s	70.5 ± 1.2	129.1 ± 0.7
10 + 5 s	70.7 ± 0.8	130 ± 0.8
10 + 10 s	74.3 ± 0.5	132 ± 0.9
10 + 20 s	76.4 ± 0.5	139.3 ± 0.5
10 + 1 min	109.3 ± 0.5	145.5 ± 0.5
10 + 5 min	113.8 ± 0.4	149.7 ± 0.5
10 + 10 min	116.6 ± 0.5	152.1 ± 0.3
15 + 3 s	59 ± 0.7	91.6 ± 1.3
15 + 5 s	59.4 ± 0.8	94.3 ± 0.8
15 + 10 s	62.1 ± 0.9	96.9 ± 0.7
15 + 20 s	66.7 ± 0.5	117.5 ± 0.5
15 + 1 min	79.5 ± 0.5	138.3 ± 0.5
15 + 5 min	100.3 ± 0.5	144.8 ± 0.4
15 + 10 min	110.3 ± 0.5	150.3 ± 0.5
20 + 3 s	39.6 ± 1.2	90.3 ± 0.5
20 + 5 s	39.7 ± 1.2	90.4 ± 0.5
20 + 10 s	56.6 ± 1.2	94.3 ± 0.8
20 + 20 s	60.6 ± 0.5	99.5 ± 0.7
20 + 1 min	69.5 ± 0.5	114.7 ± 0.5
20 + 5 min	76.5 ± 0.5	133.8 ± 0.4
20 + 10 min	92.2 ± 0.4	138.5 ± 0.5

CONCLUSIONS

In this study, we were able to produce virtually any contact angle desired on both glass and ITO substrates by controlling the specific parameters of electrospinning distance and time with a given PVP–titania precursor solution for fabricating chaotic networks of nano- and microfibers. Exhibiting very high contact angles (up to ultrahydrophobic conditions attributed to the significant fraction of loopy nanofibers), the ITO-supported fiber mats will be beneficial for any aqueous study requiring electrical connectivity, such as biosensors because the fiber mats remained stable against wetting phenomena under harsh rinsing conditions for 3 months of shelf-life and perhaps longer.

This study of fiber mats processed at 200 °C suggests that an extremely fine level of control on wettability can be accomplished as a function of the electrospinning conditions alone (Table 5), of at least 1° average uniformity in the contact angle with water or better. With the critical selection of the electrospinning substrate properties of conductivity and hydrophilicity/hydrophobicity, almost any wettability appears feasible with the resulting core–shell PVP–titania fiber networks that exhibit little variation across the mat. The correlation between increasing mat thickness and increasing contact angle appears complex and weakens substantially after complete coverage of the substrate is evident, yet the trend continues to be significant even for mats of 100 μm and more; this further suggests that the slight evolution in the electrospinning field properties as the fiber deposits grow thicker continues to affect the final outcome in the collective morphology that governs aqueous behavior, which is relevant for applications in biosensing, for example, or for the

construction of extended, three-dimensional micro- and nanostructures for cell or tissue growth.

Acknowledgment. The authors gratefully acknowledge the support of the NSF—Idaho EPSCoR Program, of the National Science Foundation under Award EPS-0447689, and of the University of Idaho Biological Applications of Nanotechnology (BANTech) Strategic Initiative.

REFERENCES AND NOTES

(1) Teo, W. E.; Ramakrishna, S. *Nanotechnology* **2006**, *17*, 89–106.
(2) Li, D.; Xia, Y. *Adv. Mater.* **2004**, *16*, 1151–1170.
(3) McCann, J. T.; Li, D.; Xia, Y. *J. Mater. Chem.* **2005**, *15*, 735–738.
(4) Li, D.; McCann, J. T.; Xia, Y. *J. Am. Ceram. Soc.* **2006**, *89*, 1861–1869.
(5) Ramakrishna, S.; Fujihara, K.; Teo, W. E.; Yong, T.; Ma, Z.; Ramaseshan, R. *Mater. Today* **2006**, *9*, 40–50.
(6) Li, D.; Ouyang, G.; McCann, J. T.; Xia, Y. *Nano Lett.* **2005**, *5*, 913–916.
(7) Yang, Y.; Jia, Z.; Hou, L.; Li, Q.; Wang, L.; Guan, Z. *IEEE Trans. Dielectr. Electr. Insul.* **2008**, *15*, 269–276.
(8) Fu, Z. W.; Ma, J.; Qin, Q. Z. *Solid State Ionics* **2005**, *176*, 1635–1640.
(9) Li, D.; Babel, A.; Jenekhe, S. A.; Xia, Y. *Adv. Mater.* **2004**, *16*, 2062–2066.
(10) Yuh, J.; Perez, L.; Sigmund, W. M.; Nino, J. C. *Physica E* **2007**, *37*, 254–259.
(11) Li, D.; Xia, Y. *Nano Lett.* **2004**, *4*, 933–938.
(12) Srivastava, Y.; Loscertales, I.; Marquez, M.; Thorsen, T. *Microfluid. Nanofluid.* **2008**, *4*, 245–250.
(13) Li, D.; Wang, Y.; Xia, Y. *Nano Lett.* **2003**, *3*, 1167–1171.
(14) Li, D.; Wang, Y.; Xia, Y. *Adv. Mater.* **2006**, *16*, 361–366.
(15) Megelski, S.; Stephens, J. S.; Chase, D. B.; Rabolt, J. F. *Macromolecules* **2002**, *35*, 8456–8466.
(16) Li, D.; Xia, Y. *Nano Lett.* **2003**, *3*, 555–560.
(17) Chandrasekar, R.; Zhang, L.; Howe, J. Y.; Hedin, N. E.; Zhang, Y.; Fong, H. *J. Mater. Sci.* **2009**, *44*, 1198–1205.
(18) Jia, C. W.; Xie, E. Q.; Zhao, J. G.; Duan, H. G. *J. Appl. Phys.* **2007**, *101*, 1–4.
(19) Lee, S. H.; Tekmen, C.; Sigmund, W. M. *Mater. Sci. Eng., A* **2005**, *398*, 77–81.
(20) Bartl, M. H.; Boettcher, S. W.; Frindell, K. L.; Stucky, G. D. *Acc. Chem. Res.* **2005**, *38*, 263–271.
(21) Shaw, D. J. *Introduction to Colloid and Surface Chemistry*, 4th ed.; Butterworth-Heinemann: Oxford, U.K., 1992; p 151.
(22) Borras, A.; Barranco, A.; Gonzalez-Elipe, A. R. *Langmuir* **2008**, *24*, 8021–8026.
(23) Watthanaarun, J.; Pavarajarn, V.; Supaphol, P. *Sci. Tech. Adv. Mater.* **2005**, *6*, 240–245.
(24) Azad, A.-M.; McKelvey, S. L.; Al-Firdaus, Z. *DoD's Adv. Mater. Manuf. Testing Inf. Anal. Center (AMMTIAC) Q.* **2008**, *3*, 3–7.
(25) Sonehara, M.; Sato, T.; Takasaki, M.; Konishi, H.; Yamasawa, K.; Miura, Y. *IEEE Trans. Magn.* **2008**, *44*, 3107–3110.
(26) Yang, Y.; Jia, Z.; Li, Q.; Guan, Z. *IEEE Trans. Dielectr. Electr. Insul.* **2006**, *13*, 580–585.
(27) Liu, Y.; Chen, J.; Misoska, V.; Wallace, G. G. *React. Funct. Polym.* **2007**, *67*, 461–467.
(28) Fischer, T.; Hampp, N. A. *IEEE Trans. Nanobiosci.* **2004**, *3*, 118–120.
(29) Tsuji, H.; Nakano, M.; Hashimoto, M.; Takashima, K.; Katsura, S.; Mizuno, A. *Biomacromolecules* **2006**, *7*, 3316–3320.
(30) Sawicka, K. M.; Prasad, A. K.; Gouma, P. I. *Sens. Lett.* **2005**, *3*, 1–5.
(31) Rojas, R.; Pinto, N. J. *IEEE Sens. J.* **2008**, *8*, 951–953.
(32) Haynes, A. S.; Gouma, P. I. *IEEE Sens. J.* **2008**, *8*, 701–705.
(33) Herricks, T. E.; Kim, S.-H.; Kim, J.; Li, D.; Kwak, J. H.; Grate, J. W.; Kim, S. H.; Xia, Y. *J. Mater. Chem.* **2005**, *15*, 3241–3245.
(34) Xie, Y.; Castracane, J. *IEEE Eng. Med. Biol. Mag.* **2009**, 23–30.
(35) Xu, Y.; Inai, R.; Kotaki, M.; Ramakrishna, S. *Biomaterials* **2004**, *25*, 877–886.
(36) Krishnappa, R. V. N.; Desai, K.; Sung, C. *J. Mater. Sci.* **2003**, *38*, 2357–2365.
(37) Hong, Y.; Ma, Z.; Wang, C.; Ma, L.; Su, M. *ACS Appl. Mater. Interfaces* **2009**, *1*, 251–256.
(38) Yang, C.; Ja, Z.; Liu, J.; Wang, K.; Guan, Z.; Wang, L.; Xu, Z. Electrical Insulation and Dielectric Phenomena. *IEEE Annual Report Conference*; Quebec City, Canada, Oct 26—29, 2008; IEEE: New York, 2008; pp 180—183.
(39) Simhan, R. G.; Moore, L. L.; Van Gunten, P. R. *J. Mater. Sci.* **1985**, *20*, 1748–1752.
(40) Zybill, C. E.; Ang, H. G.; Lan, L. L.; Choy, W. Y.; Meng, E. F. K. *J. Organomet. Chem.* **1997**, *547*, 167–172.
(41) Fukushi, Y.; Kominami, H.; Nakanishi, Y.; Hatanaka, Y. *Appl. Surf. Sci.* **2005**, *244*, 537–540.
(42) Zhong, Z.; Zhong, Y.; Liu, C.; Yin, S.; Zhang, W.; Shi, D. *Phys. Status Solidi A* **2003**, *198*, 197–203.
(43) Reneker, D. H.; Yarin, A. L. *Polymer* **2008**, *49*, 2387–2425.
(44) Ma, M.; Hill, R. M. *Curr. Opin. Colloid Interface Sci.* **2006**, *11*, 193–202.
(45) Ma, M.; Hill, R. M.; Lowery, J. L.; Fridrikh, S. V.; Rutledge, G. C. *Langmuir* **2005**, *21*, 5549–5554.

AM900481D